Optimization of reactive powder concrete by means of barite aggregate for both neutrons and gamma rays

Gökçe, H. Süleyman; Yalçınkaya, Çağlar; Tuyan, Murat

DOI
10.1016/j.conbuildmat.2018.09.022

Publication date
2018

Document Version
Accepted author manuscript

Published in
Construction and Building Materials

Citation (APA)
Gökçe, H. S., Yalçınkaya, Ç., & Tuyan, M. (2018). Optimization of reactive powder concrete by means of barite aggregate for both neutrons and gamma rays. *Construction and Building Materials*, *189*, 470-477. https://doi.org/10.1016/j.conbuildmat.2018.09.022

Optimization of reactive powder concrete by means of barite aggregate for both neutrons and gamma rays

H. Süleyman Gökçe[a*], Çağlar Yalçınkaya[b,c], Murat Tuyan[d]

[a] Bayburt University, Engineering Faculty, Civil Engineering Department, Bayburt, Turkey
[b] Dokuz Eylül University, Engineering Faculty, Civil Engineering Department, İzmir, Turkey
[c] Delft University of Technology, Faculty of Civil Engineering and Geosciences, Department of 3Md, Delft, The Netherlands
[d] İzmir Democracy University, Engineering Faculty, Civil Engineering Department, İzmir, Turkey

Abstract

High performance concrete has been often preferred in special engineering structures and in challenging composites products. Researchers have recently focused on the radiation shielding characteristics of these type concrete mixtures due to rising nuclear industry in the developing world. In the study, performance of reactive powder concrete was researched with regard to gamma-ray and neutron attenuation when its normal weight aggregate replaced with heavyweight aggregate (barite). For this purpose, reactive powder concrete mixtures were prepared 100% quartz aggregate, 100% barite aggregate and their blending 50-50%, by volume. Some physical and mechanical characteristics such as density, compressive strength, fracture energy, flexural strength and modulus of elasticity of the mixtures were determined. Gamma-ray attenuation coefficients and transmission thickness values were theoretically established for commonly known gamma energies (661.7, 1173.2 and 1332.5 keV). Optimization of the reactive powder mixtures was performed for both neutron and gamma-ray attenuation at 8 MeV. As a result, barite significantly increased the gamma-ray attenuation coefficients of reactive powder concrete. The mechanical performance of reactive powder concrete, however, was markedly reduced as a result of barite substitution. Replacement of quartz by barite aggregate has a more adverse impact on flexural strength than that of

[*]Corresponding author. Tel.: +90 (458) 333 20 33; Fax: +90 (458) 211 11 27
E-mail address: suleymangokce@bayburt.edu.tr (H. Süleyman Gökçe).

compressive strength. A mix that contains 40% barite aggregate of total aggregate volume was found as an optimum RPC mixture for simultaneously shielding neutrons and gamma rays.

Keywords: *Reactive powder concrete, barite proportion, mechanical properties, optimization, simultaneously shielding neutrons and gamma rays*

1. Introduction

Radiation has recently become one of the most famous research topics in material and physic sciences due to development of nuclear technology and spreading its use in varied industries. Moreover, interest on the alternative energy sources such as solar energy, wind power and nuclear power due to energy crisis in limited fossil fuel resources, and raise in nuclear weapon stockpile have led to irrefutable radioactive contamination in the world.

Designing and resourcing of various concrete types are essential for nuclear and medical centers against numerous applications of gamma –ray sources [1]. Several studies have been performed researching the effects of aggregate type and content, mineral admixtures, waste materials, mix proportions of normal and heavyweight concrete on their gamma-ray attenuation characteristics. Akkurt et al. [2,3,4] researched the gamma-ray shielding properties of concrete mixtures containing normal and barite aggregates. Researchers have recently focused on the alternative aggregate resources to investigate the shielding characteristics of concrete such as colemanite [5], lead mine waste [6] and lead-zinc mine waste [7]. Moreover, effect of some minor additives on the mechanical and shielding efficiency of the concrete has been researched such as boron compounds [8] and bismuth oxide additives [9]. Effect of water to cementitious materials ratio, type of aggregate and binder content on gamma-ray shielding characteristics was presented by Mostefinejad et al. [10]. Gokçe et al. [11] reported the effect of mineral admixtures, water to binder ratio, binder content on the gamma-ray attenuation properties of high consistency barite concrete mixtures.

Ouda [12] recently researched the gamma-ray shielding properties of high performance heavyweight concrete by using various aggregates.

Özen et al. [13] studied mechanical and shielding properties of high performance heavyweight concrete having low water to cement ratio (0.28) with barite aggregate and various heavyweight aggregates, and noted that increasing density improved the gamma-ray linear attenuation coefficient of the concrete mixtures. Tufekci and Gokce [14] also researched the shielding performance of heavyweight high performance fiber reinforced cementitious composites containing barite and granulated ferrous waste against X-ray and gamma-ray. Barite, a type of heavy aggregates, is generally used in heavyweight concrete production for against gamma radiation [15]. Heavyweight concrete attenuates both neutron and gamma radiation in neutron research facilities [16]. In addition to heavy elements, neutrons also need shielding materials containing light elements for elastic collisions [17]. Hu et al. [18] stated that inelastic scattering by heavy elements and elastic scattering by hydrogen are quite effective to slow down fast and intermediate-energy neutrons. Thus, the most effective shielding material for nuclear reactors can be obtained by mixing hydrogenous materials, heavy metal elements, and other neutron absorbers [19]. Akkurt and El-Khayatt [20] showed that an optimum barite content of normal performance concrete was more effective for shielding both neutron and gamma-ray.

Thanks to its superior mechanical and durability performance, reactive powder concrete (RPC), a type of ultra-high performance concrete, was suggested for industrial and nuclear waste storage facilities by Richard and Cheyrezy [21]. Özen et al. [13] reported that structures accommodating radiation-emitting devices require not only adequate shielding against radiation, but also strength properties. Researchers have recently tried to improve physical and mechanical properties, fire resistance, etc. characteristics of RPC by means of various mix design parameters [22-28]. However, due to high heat of hydration and shrinkage problems [29,30], RPC should be considered in modular precast products rather than massive constructions in-situ applications. Thereby, the products can be evaluated as an alternative shielding material by optimizing its mix components for simultaneously shielding neutrons and gamma rays.

In this study, RPC mixtures were produced by the replacement of its conventional aggregate (quartz) with barite aggregate at 0, 50 and 100%, by volume. Detailed mechanical properties and shielding characteristics of RPC mixtures were determined. In addition to determination of commonly used attenuation coefficients and attenuation thicknesses of the mixtures at 661.7, 1173.2 and 1332.5 keV energies of gamma rays, optimum barite proportion was theoretically found for both neutrons and gamma rays at 8 MeV.

2. Experimental study

2.1. Materials

Some chemical and physical properties of Portland cement (CEM I 42.5 R) and silica fume used in this study are presented in Table 1. To approximate particle size distribution of 0 – 1 mm barite aggregate, quartz aggregate skeleton was composed by 0 – 0.4 mm (40%) and 0.5 – 1 mm (60%) grain sizes. The density and water absorption properties of quartz and barite aggregate are 2.65 kg/dm^3 and 0.12%, and 4.08 kg/dm^3 and 0.54%, in sequence. Oxide composition and grading curve of aggregates are given in Table 2, and Fig. 1, respectively. A polycarboxylate based superplasticizer was used in this study. A straight type, brass coated steel micro-fiber with a 13 mm length, 0.20 mm diameter and an aspect ratio as 65 was used as reinforcing material. The density and tensile strength of steel micro-fiber are 7.17 kg/dm^3 and 2750 MPa, respectively.

Table 1. Some chemical and physical properties of cement and silica fume

Chemical composition (wt.%)	Cement	Silica fume
CaO	61.85	0.49
SiO_2	19.1	92.26

Al_2O_3	4.40	0.89
Fe_2O_3	3.96	1.97
MgO	2.05	0.96
Na_2O	0.27	0.42
K_2O	0.70	1.31
SO_3	3.72	0.33
Cl^-	0.0004	0.09
Loss on ignition	1.82	-
Physical properties		
28-day strength activity index (%)	-	95
Fineness (m^2/kg)*	369	20000
Specific gravity	3.12	2.2

* Nitrogen absorption method for SF, Blaine method for the others.

Table 2. Oxide composition of aggregates

Oxides (wt.%)	Barite	Quartz
$BaSO_4$	74.31	-
SiO_2	14.80	92.26
Fe_2O_3	0.53	1.97
Al_2O_3	4.67	0.89
CaO	1.06	0.49
K_2O	0.85	1.31
MgO	0.42	0.96
P_2O_5	0.07	-
MnO	0.25	-
SrO	0.75	-
V_2O_5	1.17	-
Nd_2O_3	0.83	-
Ta_2O_5	0.01	-
Sc_2O_3	0.09	-
Sm_2O_3	0.08	-

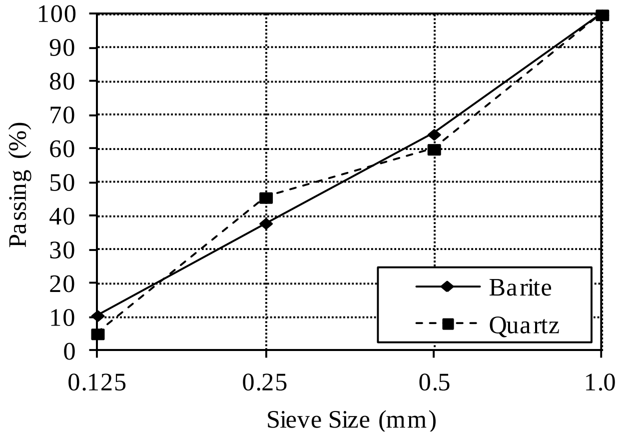

Fig. 1. Grading curve of aggregates

To evaluate the effect of replacement of quartz by barite aggregate, three RPC mixtures were prepared. These mixtures were denoted as Q, Q+B, and B depending on the aggregate source. Q and B mixtures were completely composed of quartz and barite aggregate in sequence, whereas Q+B mixture was composed of 50% quartz and 50% barite combination by volume. Note that all RPC mixtures have an aggregate volume of 35%. The aggregate volume of RPC should be limited to ensure ultra-high strength with enough workability.

2.2. Methods and Analyses

A special mixing procedure was followed to obtain a homogenous RPC matrix. First of all, cement and silica fume were mixed. Thereafter, the mix water with superplasticizer was added to the dry mix. After fluidization of the paste, aggregates were added to the wet mixture. The final mixing was applied for 10 min at high-speed rotation. The mixtures were poured into cylindrical and prismatic moulds with dimensions of 100×200 mm, and 40×40×160 mm, respectively. The RPC mixtures were poured into the moulds in three layers, and each layer was compacted by external vibration without rodding. Note that the flow test was carried out in accordance with ASTM C1437 [31]. All mixtures exhibited 170±5 mm of flow diameter at the same superplasticizer dosage. The mix proportions can be seen in Table 3.

Table 3. Mix proportions

Materials (kg/m^3)	Mixtures		
	Q	Q+B	B
Water	190	190	190
Portland cement	906	906	906
Silica fume	227	227	227
0 – 1 mm quartz	939	469	-
0 – 1 mm barite	-	723	1444
Steel micro-fiber	143.4	143.4	143.4
Superplasticizer	23	23	23
Design parameters			
Barite/total aggregate (%, by volume)	0	50	100
Paste volume (%)	65	65	65
Water/cement*	0.22	0.22	0.22

Water/binder*	0.18	0.18	0.18

*includes additional water from superplasticizer

The physical and mechanical performances of the mixtures were evaluated after steam curing. The molded specimens were kept in the laboratory condition at 20±1 °C and 60±5% relative humidity during first 24-hour. Heating period was started after the 24-hour delay period. The temperature of the cabin reached 90°C within six hours and the demoulded specimens were kept in this temperature for 65 hours to achieve ultimate strength of designed mixtures. A gradual cooling period was applied to avoid thermal shock cracking of RPC.

Density and volume of free water of hardened RPC specimens (Ø100×200 mm) were taken into account for the calculation of their attenuation properties. Density values of the specimens were determined in oven-dry condition according to EN 12390-7 [32]. Moreover, the volume of free water was calculated as a percent of total specimen volume by using Eq. (1).

$$V = [(WS-OD) / (WS-MW)] \times 100 \quad (1)$$

where, V: volume of free water (%), WS: mass of water saturated specimen (kg), OD: mass of oven-dried specimen (kg), MW: mass of specimen in water (kg).

The load-deflection graph of the mixture was obtained with carrying out three-point bending tests by an electro-mechanic closed-loop testing system on four 40×40×160 mm prismatic specimens in accordance with Japan Concrete Institute Standard [33]. Thus, loading span, notch depth, and loading rate were 120 mm, 12 mm, and 0.1 mm/min, in sequence. The mid-span deflection was recorded up to 2.0 mm. The fracture energy was calculated by dividing the area under the load-deflection curve by the effective cross-section area for each specimen. Note that due to the small prismatic specimens were tested, the weight of these specimens was neglected in the calculation of fracture energy. Compressive strength tests were performed on eight pieces (40×40×40 mm) left from flexural test of 40×40×160 mm specimens according to

ASTM C349 [34] for each mixture. Modulus of elasticity was determined on cylindrical specimens (Ø100×200 mm) according to ASTM C 469M [35] from the stress–strain curve up to the 35% of maximum stress.

2.3. Attenuation of gamma rays

The mass attenuation coefficients (μ_m) of RPC mixtures were theoretically calculated with the help of the XCOM program developed by Berger et al. [36]. The program calculates the mass attenuation coefficients according to the chemical composition of the materials. The elemental ingredients of the hardened concrete were calculated by considering experimental results (oven-dry density and volume of free water) and given in Table 4.

Table 4. Relative elemental ingredients of hardened mixes

Elements	Atomic number (Z)	Mix Q	Mix Q+B	Mix B
H	1	0.074318	0.067244	0.061508
O	8	0.395989	0.351549	0.314936
Na	11	0.001141	0.001006	0.000895
Mg	12	0.005426	0.005588	0.005722
Al	13	0.009710	0.015462	0.020198
Si	14	0.258427	0.170090	0.097337
S	16	0.005971	0.033248	0.055700
K	19	0.003350	0.004940	0.006247
Ca	20	0.173808	0.159261	0.147315
Sc	21	0.000000	0.000160	0.000291
V	23	0.000000	0.001786	0.003256
Cr	24	0.000755	0.000683	0.000624
Mn	25	0.000000	0.000528	0.000962
Fe	26	0.069595	0.063973	0.059320
Sr	38	0.000000	0.001728	0.003151
Ba	56	0.000000	0.119258	0.217413
Nd	60	0.000000	0.001939	0.003535
Sm	62	0.000000	0.000188	0.000343
W	74	0.001509	0.001366	0.001248
Total		0.999999	0.999997	1.000001
Moderator fraction (Z≤16)		0.750982	0.644187	0.556296
Density, g/cm^3		2.438	2.684	2.943
Volume of free water, %		0.95	1.14	1.25

Gamma-ray linear attenuation coefficients were calculated by using the hardened densities of the mixtures according to Eq. (2). Moreover, the relation between transmission and absorber thickness was constituted in logarithmic scale, and their mean free path (MFP), half-value layer (HVL) and tenth-value layer (TVL) were determined by using Eq. (3), Eq. (4) and Eq. (5), respectively.

$$\mu = \mu_m \times \gamma \quad (2)$$

$$MFP = 1/\mu \quad (3)$$

$$HVL = \ln 2/\mu \quad (4)$$

$$TVL = \ln 10/\mu \quad (5)$$

where, μ: linear attenuation coefficient (cm^{-1}), μ_m: mass attenuation coefficient (cm^2/g), γ: concrete density (g/cm^3)

2.4. Attenuation of neutrons

Buildup factor that allows colliding neutrons and still escaping simplifies the reasonably accurate calculation of attenuation for shields containing moderating materials at 8 MeV. Moderating materials that are elements with low atomic number (≤16) slow down and absorb neutrons [37]. Thus, neutron attenuation coefficients of RPC mixtures were theoretically calculated with the help of the online NCNR [38] computation program at 8 MeV. Wavelength was selected as 1.01121×10^{-4} Å to test the aforementioned energy of fast neutrons in the computation.

Relationships between gamma-ray and neutron attenuation coefficients were assessed, and the coefficients were related with mechanical properties, moderator fractions, density values and barite contents of RPC mixtures.

3. Results and Discussion

3.1. Mechanical properties

Load-deflection curve of the mixtures obtained by three-point bending test can be seen in Fig. 2. The gradual load decrement was observed in all mixtures after the peak load. High post peak load-carrying capacity shows well fracture energy and reinforcing effect of the steel fibers. The formation of deflection hardening after the first crack is a typical indication of high performance. The highest peak load was exhibited by traditional RPC composed of quartz as aggregate phase. Inclusion of barite aggregate decreased the peak loads achieved. The lowest performance was exhibited by RPC consisting only of barite aggregate. This can be attributed to silica flour of quartz that enhances steel fiber-matrix bond characteristics. In addition, this considerable reduction in the performance due to barite inclusion was explained by the friability of barite during mixing as well as interface transition zone deficient [39]. Even if the deflection was at 2.0 mm, the flexural load carried by the specimens was 57-67% of the ultimate load measured for all mixtures.

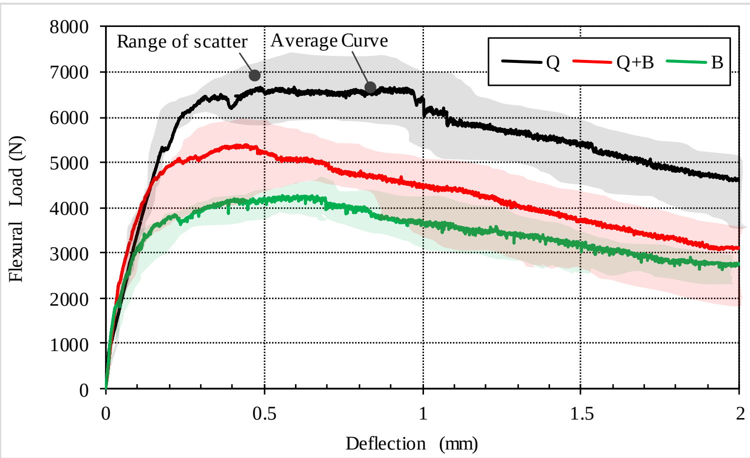

Fig. 2. Flexural load - deflection curves of the mixtures

Flexural strength of the RPC mixtures is shown in Fig. 3(a). Q, Q+B, and B mixtures have exhibited flexural strength of 40, 31.4, and 25.5 MPa, respectively. Note that four specimens were tested for each mixture. It can be seen from Fig. 2 that, however, there is an important scatter on the load-deflection curves depending on distribution and orientation of steel fibers [40]. Thus, a non-negligible standard deviation for flexural strength up to 4.5 MPa was obtained. 50% barite replacement reduced the flexural strength of RPC by 22%. When the replacement ratio was 100%, the reduction was recorded by 36%. Due to barite replacement, both a reduction in quartz powder, thereby in steel fiber-matrix characteristics, and a reduction in robustness of aggregate phase itself affected negatively the performance under flexural loads. This decrement can be seen in the fracture energies under flexural loading as expected. Reduction in fracture energies under flexural loads was a bit higher than loss of flexural strength.

One of the most outstanding properties of RPC is its higher compressive strength compared to that of other cementitious composites. This can be attributed to low water to cement ratio, and high cementitious material content of it as well as well-designed micro skeleton concerning packing. As can be seen in Fig. 3(b), a compressive strength level of 218 MPa was reached by traditional RPC mixture with quartz aggregate skeleton. 50% and 100% replacement of quartz by barite caused a compressive strength reduction of 13%, and 21%, respectively. Compressive strength reduction due to barite substitution can be attributed to four possible reasons: less compressive strength of barite than that of quartz, less quartz powder that enhances interfacial transition zones in RPC, reduction in the bond properties between aggregates and matrix due to weak particles around the barite [39], and as observed in the study of González-Ortega et al. [41] even for a normal mixing procedure, the friability of barite aggregate during drastic mixing procedure of RPC. The variations of moduli of elasticity were found similar to those of the compressive strength values of RPC mixtures. The modulus of elasticity of RPC mixture with 100% barite aggregate was found 16% less than the modulus of elasticity of RPC mixture with 100% quartz aggregate. This can be resulted by weaker interfacial transition zone between barite aggregate and paste [39].

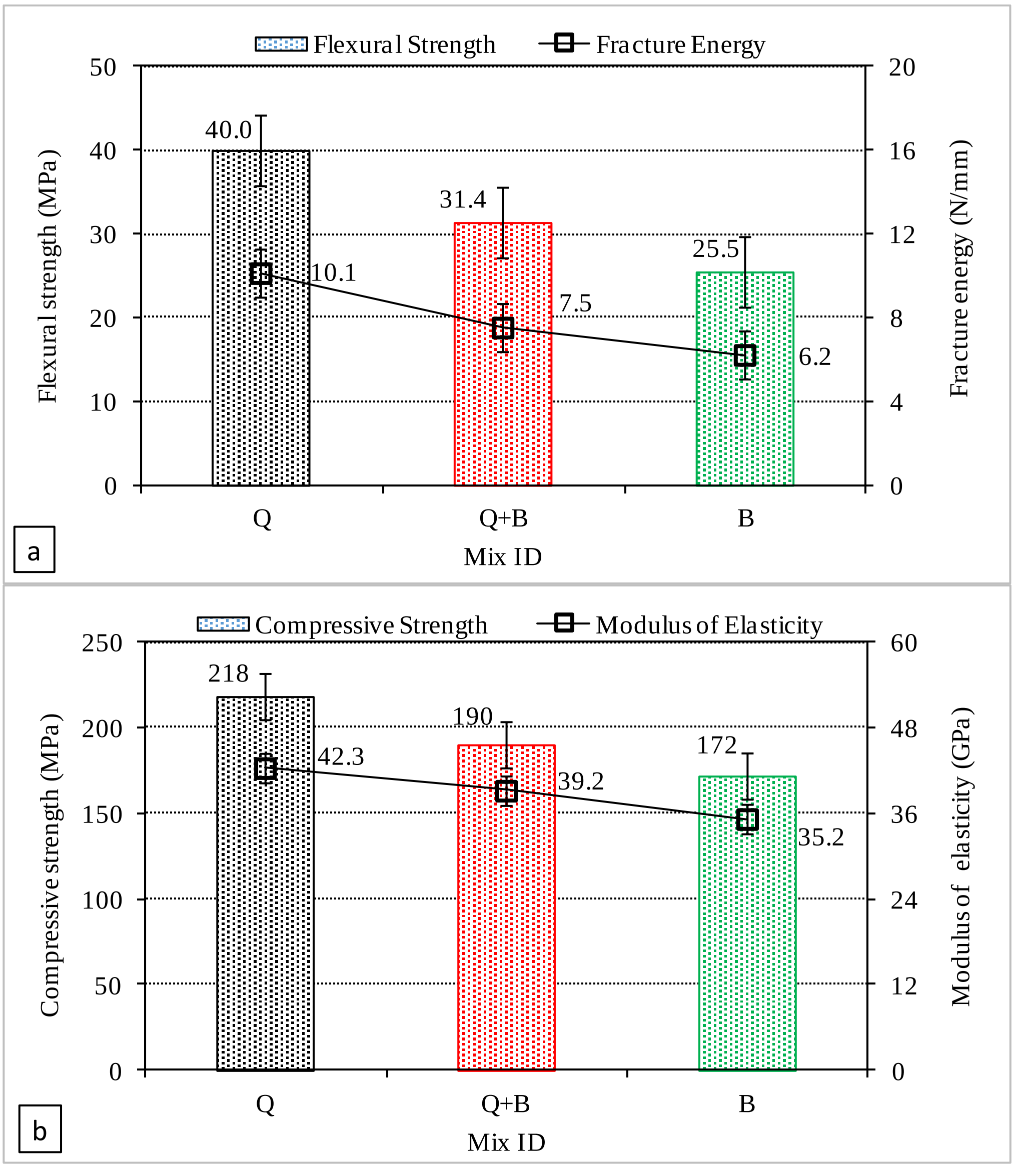

Fig. 3. Flexural strength and fracture energy (a), compressive strength and modulus of elasticity (b) of RPC mixtures

3.2. Gamma-ray attenuation coefficients

Theoretical total mass attenuation coefficients with coherent scattering are given in Fig. 4(a) for gamma energies between 0.001 and 100000 MeV. The introduction of barite into the RPC mixtures increased the total attenuation coefficients below 0.3 MeV and above 8 MeV gamma energies because photo-electric and pair production effect can be occurred by the increase of atomic number of matter, respectively, as reported by Knoll [42] and Tsoulfanidis [43]. ^{137}Cs and ^{60}Co, well-known radionuclides, are commonly used in calibration of nuclear detectors, sterilization, medical therapy and applications, in gauges for measuring liquid flows and thickness of materials, as a radiation source in radiography, etc. [1]. Mass attenuation coefficients of RPC mixtures at the certain gamma energies (661.7, 1173.2 and 1332.5 keV) of ^{137}Cs and ^{60}Co are given in Fig. 4(b). It is understood that the coefficients were slightly decreased by increasing concrete density at higher barite content. RPC mixture containing 100% barite aggregate showed 1.1, 3.5 and 3.6% less mass attenuation coefficient than those of RPC mixture without barite at 661.7, 1173.2 and 1332.5 keV, respectively. For a given gamma-ray energy, the mass attenuation coefficient is not changed due to the physical state variations of a given absorber [42].

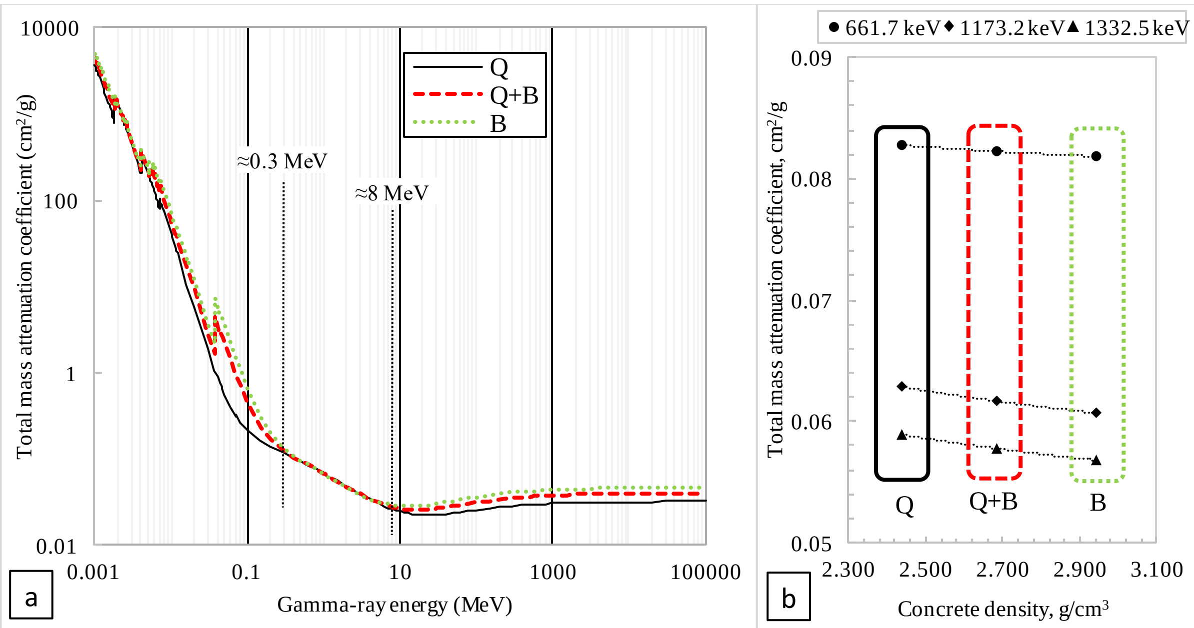

Fig. 4. Total mass attenuation coefficients vs. gamma-ray energy (a), total mass attenuation coefficients vs. concrete density (b) (1 MeV=1000 keV)

Fig. 5 presents the linear attenuation coefficients of RPC mixtures at the selected gamma energies. While there is no remarkable effect of barite on mass attenuation coefficients (≤3.6% reduction), the linear attenuation coefficients of RPC increased up to 19% thanks to remarkable increase of density values by addition of barite. The increments were found more remarkable at high energy of gamma rays (1332.5 keV). Akkurt et al. [4] was also found the similar increment (16%) in normal performance concrete when fully replaced of its calcite aggregate by barite aggregate.

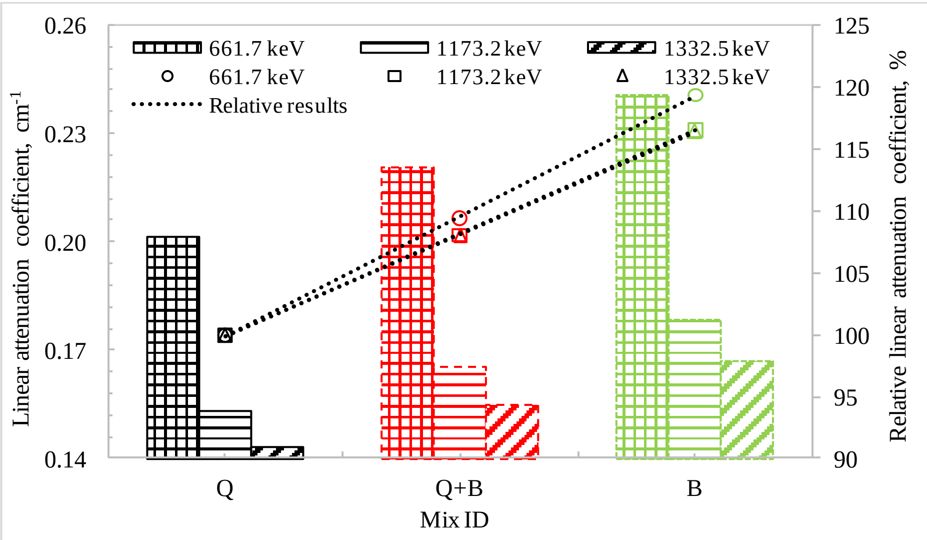

Fig. 5. Gamma-ray linear attenuation coefficients for certain gamma energies

3.3. Transmission thicknesses of gamma rays

The relationships between the transmission of the gamma rays and the shielder (RPC) thickness were established in Fig. 6 at 661.7 keV, 1173.2 keV and 1332.5 keV energies. Moreover, mean free path, half- and tenth-value layers that are the mostly used transmission layers of the gamma rays in shield design are given for each gamma energy in Fig. 7. The attenuation thickness of the RPC mixtures decreased with increasing of barite content. Similarly, Zorla et al. [44] recently reported that the attenuation thickness of concrete increased with increasing in gamma-ray energy and slightly reduced at low energies of gamma rays (from 100 to 1000 keV).

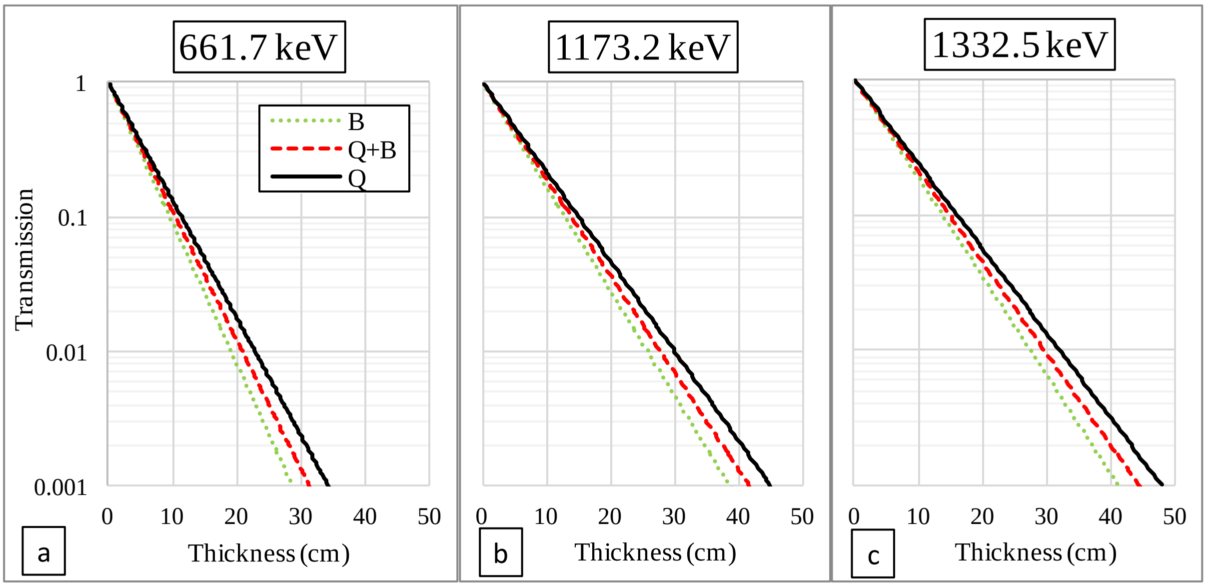

Fig. 6. Relationships between transmission of gamma rays and thickness of RPC

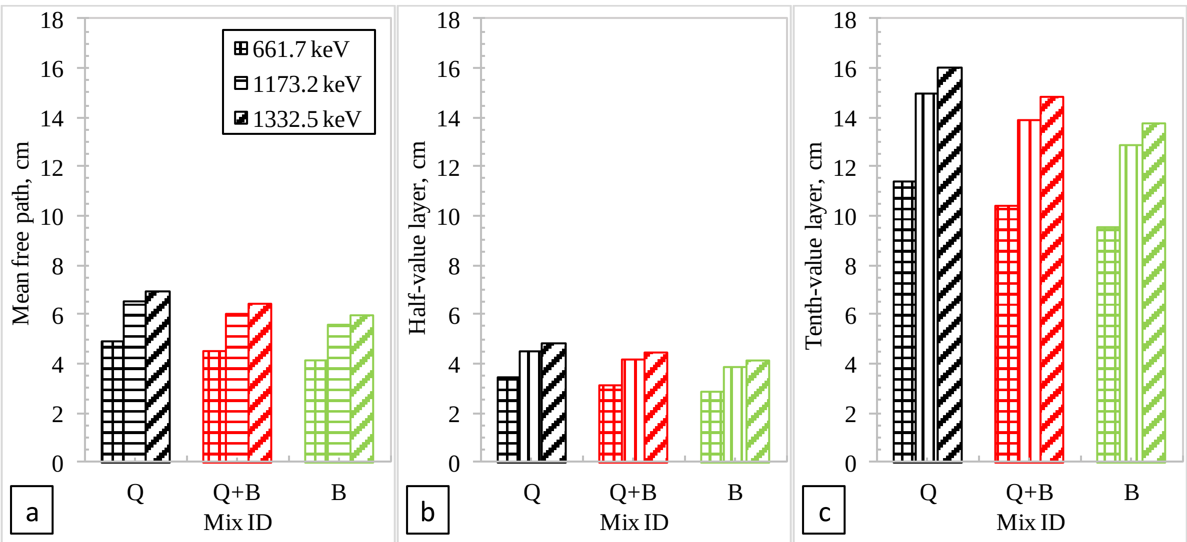

Fig. 7. Some selected attenuation thicknesses for mean free path (a), half-value layer (b), and tenth-value (c) layer

3.4. Relationships between linear attenuation coefficients and mechanical properties

Fig. 8 presents linear relationships between linear attenuation coefficients and mechanical properties for particular energy of 8 MeV. It can be seen that the linear relationships were very strong for the mechanical properties under compression or flexure. Gamma-ray attenuation coefficients were reduced by increasing mechanical properties of RPC by contrast with neutron attenuation coefficients. This is mainly because increasing the barite substitution, which enhances gamma-ray attenuation of RPC by means of increasing the density, adversely affected the mechanical properties in this study. On the other hand, Al-Humaiqani et al. [45] reported that an increase in compressive strength of high performance heavyweight concrete containing only heavyweight aggregate (barite or hematite) could be improved gamma-ray attenuation coefficients. Moreover, it seems that even if steel fiber usage can increase the mechanical properties [14] and gamma-ray attenuation coefficient of RPC [46], the adverse effect of replacing quartz by barite on the compressive strength, modulus of elasticity, flexural strength, and fracture energy could not be prevented. Thus, barite content of RPC mixture designed for radiation shielding purposes should be optimized for both gamma rays and neutrons by considering the losses in mechanical properties.

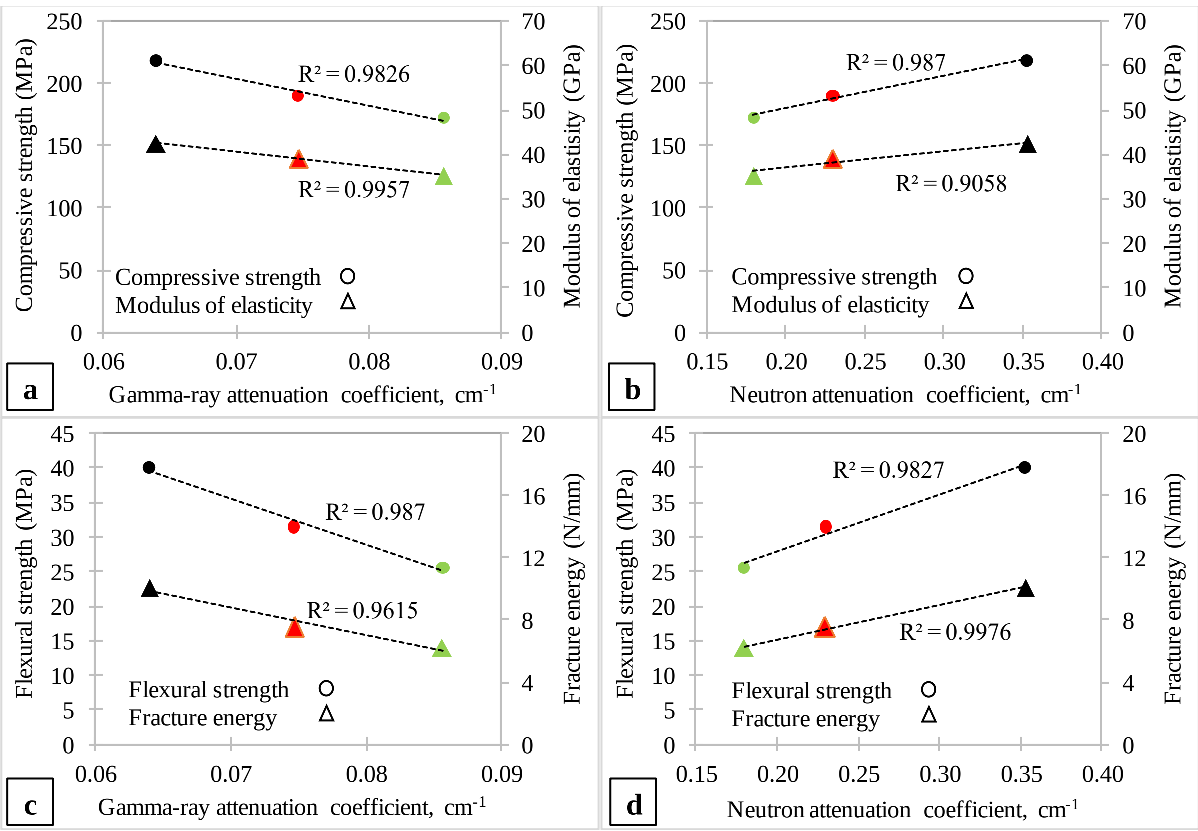

Fig. 8. Relationships between gamma-ray attenuation coefficient and compressive strength or modulus of elasticity (a), neutron attenuation coefficient and compressive strength or modulus

of elasticity (b), gamma-ray attenuation coefficient and flexural strength or fracture energy (c), neutron attenuation coefficient and flexural strength or fracture energy (d)

3.5. Optimization of RPC mixtures for both neutrons and gamma rays

Polynomial relations established between moderator fraction or density or barite content and linear attenuation coefficients of both neutrons and gamma rays are given at 8 MeV in Fig. 9. It was found that there is exactly opposite variation for neutron and gamma-ray attenuation coefficients according to the mixing parameters. That is, gamma-ray attenuation coefficients of the RPC mixtures were increased with decreasing moderator fraction, and with increasing of density and barite content, exactly unlike to the relations for neutron attenuation coefficients. Similarly, Gencel et al. [47] reported that desired gamma-ray attenuation coefficients were found by replacement of hematite aggregate, while there was no positive effect on neutron shielding due to reducing hydrogen content in denser concrete mixtures. Moreover, El-Khayatt and Akkurt [48] stated that decrease of moderator fraction was reduced the neutron attenuation coefficients. Therefore, an optimum moderator fraction, density or barite content can be suggested to balance shielding capability of RPC efficiently against the both types of radiation. As a result, RPC mixture having 40% barite-60% quartz aggregate gives better shielding characteristics for both neutrons and gamma rays in the study. The optimum proportion was recommended as 54% barite for simultaneous protection against neutrons and gamma rays in normal performance concrete by Akkurt and El-Khayatt [20].

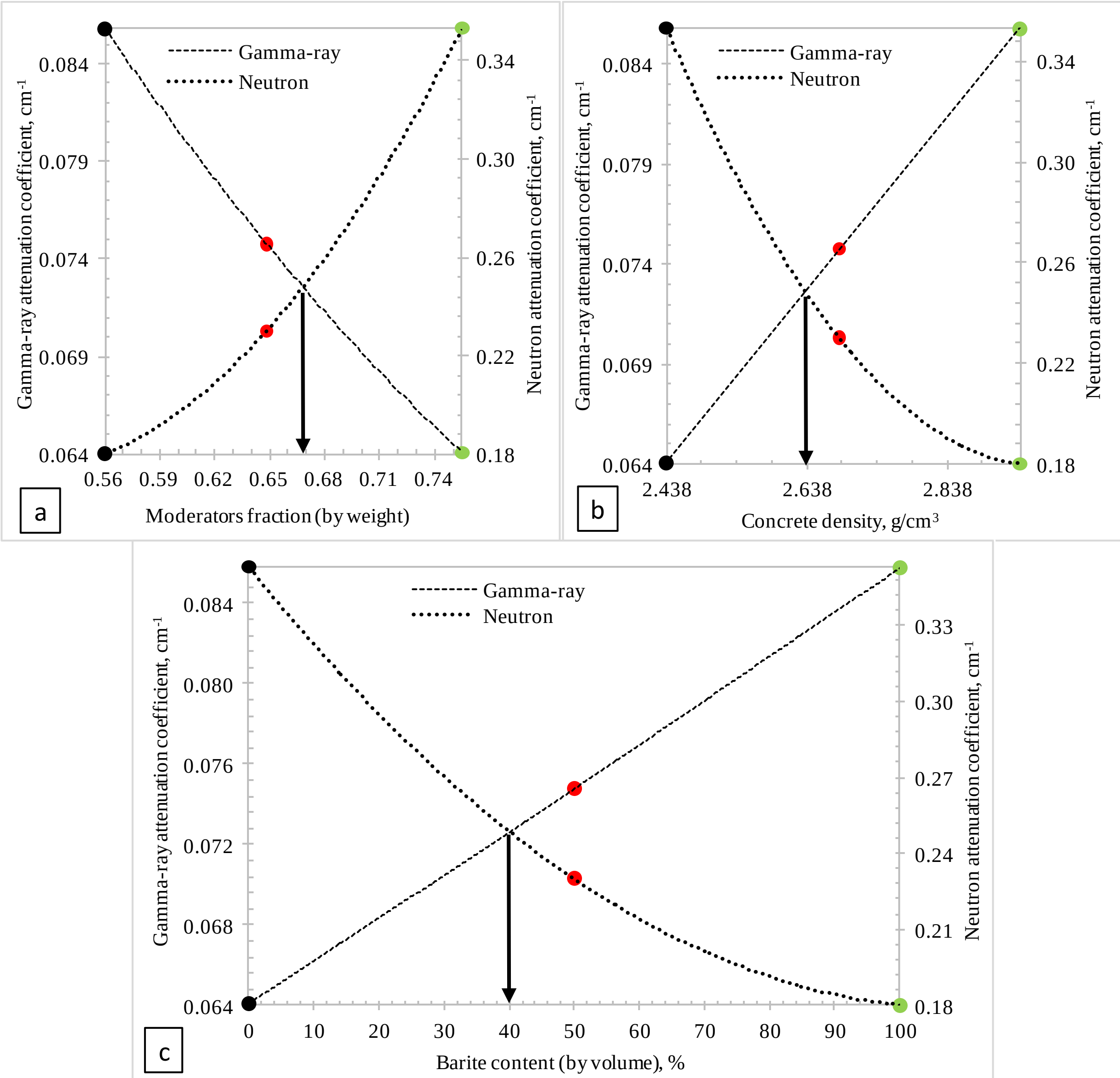

Fig. 9. Relationships between attenuation coefficients and moderator fractions (a), concrete density values (b), barite contents (c)

4. Conclusions

Recent studies emphasize that optimization of mix proportions is required for efficiently attenuation of gamma rays accompanied by neutrons. The following conclusions of reactive powder concrete mixtures can be drawn about mechanical characteristics and shielding gamma rays and neutrons in this study:

- The mechanical performance of RPC with barite aggregate was significantly lower than that of RPC with quartz aggregate. Replacement of quartz by barite aggregate has a more adverse impact on flexural strength than that of compressive strength. Thus, the optimization of aggregate proportions can moderate the loss in mechanical properties in addition to its shielding benefits.

- Barite increased the gamma-ray mass attenuation coefficients of reactive powder concrete mixtures below 0.3 MeV and above 8 MeV energies. The mass attenuation coefficients were slightly reduced out of the energies as seen at 661.7, 1173.2 and 1332.5 keV energies of gamma rays.
- Linear attenuation coefficient was significantly increased (up to 19%) by the use of barite, and thus, the attenuation thickness of reactive powder concrete was reduced for certain gamma-ray transmission.
- The linear gamma-ray attenuation coefficients were increased by decreasing linear neutron attenuation coefficients. Gamma-ray attenuation coefficients were reduced by increasing mechanical properties of RPC by contrast with neutron attenuation coefficient. The relations show that barite content of RPC should be meticulously proportioned without overlook the mechanical characteristics.
- Attenuation coefficients for neutrons and gamma rays at 8 MeV showed opposite relation for moderator fraction, density and barite content of RPC. Thereby, 40% barite-60% quartz aggregate combination is suggested for the production of RPC for simultaneous shielding neutrons and gamma rays in the study.
- Authors of the study recommend the optimum selection of aggregate proportions according to individual combinations of radiation types and energies in any concrete production.

References

[1] S.P. Shirmardi, M. Shamsaei, M. Naserpour, Comparison of photon attenuation coefficients of various barite concrete and lead by MCNP code, XCOM and experimental data, Ann. Nucl. Energy 55 (2013) 288-291.

[2] I. Akkurt, C. Basyigit, S. Kilincarslan, B. Mavi, The shielding of ɣ-rays by concretes produced with barite, Prog. Nucl. Energy 46 (2005) 1-11.

[3] I. Akkurt, C. Basyigit, S. Kilincarslan, B. Mavi, A. Akkurt, Radiation shielding of concretes containing different aggregates, Cem. Concr. Compos. 28 (2006) 153-157.

[4] I. Akkurt, H. Akyıldırım, B. Mavi, S. Kilincarslan, C. Basyigit, Photon attenuation coefficients of concrete includes barite in different rate, Ann. Nucl. Energy 37 (2010) 910-914.

[5] F. Demir, G. Budak, R. Sahin, A. Karabulut, M. Oltulu, A. Un, Determination of radiation attenuation coefficients of heavyweight- and normal-weight concretes containing colemanite and barite for 0.663 MeV γ-rays, Ann. Nucl. Energy 38 (2011) 1274-1278.

[6] M. Çullu, H. Erbaş, Determination of the effect of lead mine waste aggregate on some concrete properties and radiation shielding, Constr. Build. Mater. 125 (2016) 625-631.

[7] M. Çullu, E. Bakırhan, Investigation of radiation absorption coefficients of lead-zinc mine waste rock mixed heavy concrete at 662–1460 keV energy range, Constr. Build. Mater. 173 (2018) 17-27.

[8] M.H. Kharita, S. Yousef, M. AlNassar, Review on the addition of boron compounds to radiation shielding concrete, Prog. Nucl. Energy 53 (2011) 207-211.

[9] Y. Yao, X. Zhang, M. Li, R. Yang, T. Jiang, J. Lv, Investigation of gamma ray shielding efficiency and mechanical performances of concrete shields containing bismuth oxide as an environmentally friendly additive, Radiat. Phys. Chem. 127 (2016) 188-193.

[10] D. Mostofinejad, M. Reisi, A. Shirani, Mix design effective parameters on γ-ray attenuation coefficient and strength of normal and heavyweight concrete, Constr. Build. Mater. 28 (2012) 224-229.

[11] H.S. Gökçe, B. Canbaz Öztürk, N.F. Çam, Ö. Andiç Çakır, Gamma-ray attenuation coefficients and transmission thickness of high consistency heavyweight concrete containing mineral admixture, Cem. Concr. Compos. 92 (2018) 56-69.

[12] A.S. Ouda, Development of high-performance heavy density concrete using different aggregates for gamma-ray shielding, Prog. Nucl. Energy 79 (2015) 48-55.

[13] S. Özen, C. Şengül, T. Erenoğlu, Ü. Çolak, İ.A. Reyhancan, M.A. Taşdemir, Properties of heavyweight concrete for structural and radiation shielding purposes, Arab. J. Sci. Eng. 41 (2016) 1573-1584.

[14] M.M. Tufekci, A. Gokce, Development of heavyweight high performance fiber reinforced cementitious composites (HPFRCC) – Part II: X-ray and gamma radiation shielding properties, Constr. Build. Mater. 163 (2018) 326-336.

[15] S.Y. Lee, A.M. Daugherty, D.J. Broton, Assessing aggregates for radiation-shielding concrete, Concr. Int. 35 (2013) 31-38.

[16] E. Calzada, F. Grünauer, B. Schillinger, H. Türck, Reusable shielding material for neutron- and gamma-radiation, Nucl. Instr. Meth. Phys. Res. A. 651 (2011) 77-80.

[17] P.K. Mehta, P.J.M., Monteiro, Concrete: Microstructure, Properties, and Materials (3. Edition), McGraw-Hill, USA, 2006.

[18] H. Hu, Q. Wang, J. Qin, Y. Wu, T. Zhang, Z. Xie, X. Jiang, G. Zhang, H. Xu, X. Zheng, J. Zhang, W. Liu, Z. Li, B. Zhang, L. Li, Z. Song, X. Ouyang, J. Zhu, Y. Zhao, X. Mi, Z. Dong, C. Li, Z. Jiang, Y. Zhan, Study on composite material for shielding mixed neutron and γ-rays, IEEE Trans. Nucl. Sci. 55 (2008) 2376-2384.

[19] A.M. El-Khayatt, A program for calculating attenuation coefficients of fast neutrons and gamma-rays, Ann. Nucl. Energy 38 (2011) 128-132.

[20] I. Akkurt, A.M. El-Khayatt, The effect of barite proportions on neutron and gamma-ray shielding, Ann. Nucl. Energy 51 (2013) 5-9.

[21] P. Richard, M. Cheyrezy, Composition of reactive powder concrete, Cem. Concr. Res. 25 (1995) 1501-1511.

[22] S. Bhanja, B. Sengupta, Influence of silica fume on the tensile strength of concrete, Cem. Concr. Res. 35 (2005) 743-747.

[23] H. Yazıcı, M.Y. Yardımcı, S. Aydın, A.Ş. Karabulut, Mechanical properties of reactive powder concrete containing mineral admixtures under different curing regimes, Constr. Build. Mater. 23 (2009) 1223-1231.

[24] Y. Ju, H. Liu, G. Sheng, H. Wang, Experimental study of dynamic mechanical properties of reactive powder concrete under high-strain-rate impacts, Sci. China Technol. Sc. 53 (2010) 2435-2449.

[25] Y.S. Tai, H.H. Pan, Y.N. Kung, Mechanical properties of steel fiber reinforced reactive powder concrete following exposure to high temperature reaching 800 °C, Nucl. Eng. Des. 241 (2011) 2416-2424.

[26] W. Zheng, B. Luo, Y. Wang, Compressive and tensile properties of reactive powder concrete with steel fibres at elevated temperatures, Constr. Build. Mater. 41 (2013) 844-851.

[27] S. Ahmad, A. Zubair, M. Maslehuddin, Effect of key mixture parameters on flow and mechanical properties of reactive powder concrete, Constr. Build. Mater. 99 (2015) 73-81.

[28] Y. Ju, K. Tian, H. Liu, H.W. Reinhardt, L. Wang, Experimental investigation of the effect of silica fume on the thermal spalling of reactive powder concrete, Constr. Build. Mater. 155 (2017) 571-583.

[29] E. Erten, C. Yalcinkaya, A. Beglarigale, H. Yigiter, H. Yazici, Effect of early age shrinkage cracks on the corrosion of rebar embedded in ultra high performance concrete with and without fibers, J. Fac. Eng. Archit. Gazi Univ. 32 (2017) 1347-1364.

[30] C. Yalcinkaya, H. Yazici, Effect of ambient temperature and relative humidityon early-age shrinkage of UHPC with high-volume mineral admixtures, Constr. Build. Mater. 144 (2017) 252-259.

[31] ASTM C1437-15, Standard test method for flow of hydraulic cement mortar, ASTM International, West Conshohocken, PA, 2015, www.astm.org

[32] EN 12390-7, Testing hardened concrete-Part 7: Density of hardened concrete, European Committee for Standardization, 2009.

[33] Japan Concrete Institute, Method of test for load-displacement curve of fiber reinforced concrete by use of notched beam, 2003.

[34] ASTM C349-14, Standard test method for compressive strength of hydraulic-cement mortars (Using portions of prisms broken in flexure), West Conshohocken, PA, 2014, www.astm.org

[35] ASTM C469, Standard test method for static modulus of elasticity and poisson's ratio of concrete in compression, ASTM International, West Conshohocken, PA, 2010, www.astm.org

[36] M.J. Berger, J.H. Hubbell, S.M. Seltzer, J. Chang, J.S. Coursey, R. Sukumar, D.S. Zucker, K. Olsen, NBSIR 87-3597, Photon cross sections on a personal computer, National Institute of Standards, USA, 1998. http://physics.nist.gov/PhysRefData/Xcom/Text/XCOM.html, (accessed 28.03.2018)

[37] NCRP (National Committee on Radiation Protection and Measurements), Protection against Neutron Radiation up to 30 Million Electron Volts. Report No. 20., NBS Handbook 63, National Bureau of Standards, USA, 1957.

[38] NCNR, Compute neutron attenuation and activation, NIST Center of Neutron Research, USA, 2005. https://www.ncnr.nist.gov/index.html, (accessed 01.04.2018)

[39] K. Saidani, L. Ajam, M.B. Ouezdou, Barite powder as sand substitution in concrete: Effect on some mechanical properties, Constr. Build. Mater. 95 (2015) 287-295.

[40] S.J. Barnett, J.F. Lataste, T. Parry, S.G. Millard, M.N. Soutsos, Assessment of fibre orientation in ultra high performance fibre reinforced concrete and its effect on flexural strength, Mater. Struct. 43 (2010) 1009-1023.

[41] M.A. González-Ortega, S.H.P. Cavalaro, A. Aguado, Influence of barite aggregate friability on mixing process and mechanical properties of concrete, Constr. Build. Mater. 74 (2015) 169-175.

[42] G.F. Knoll, Radiation Detection and Measurement (3. Edition), John Wiley and Sons Inc., USA, 1999.

[43] N. Tsoulfanidis, Measurement and Detection of Radiation (2. Edition), Taylor and Francis, USA, 1995.

[44] E. Zorla, C. Ipbüker, A. Biland, M. Kiisk, S. Kovaljov, A.H. Tkaczyk, V. Gulik, Radiation shielding properties of high performance concrete reinforced with basalt fibers infused with natural and enriched boron, Nucl. Eng. Des. 313 (2017) 306-318.

[45] M.M. Al-Humaiqani, A.B. Shuraim, R.R. Hussain, Effect of compressive strength on γ-radiation attenuation coefficients for high performance concrete, IACSIT Int. J. Eng. Technol. 5 (2013) 566-572.

[46] S.D. Mohammed, W.Z. Majeed, N.B. Naji, N.M. Fawzi, Investigating the influence of gamma ray energies and steel fiber on attenuation properties of reactive powder concrete, Nucl. Sci. and Tech. 28 (2017) 153.

[47] O. Gencel, A. Bozkurt, E. Kam, T. Korkut, Determination of calculation of gamma and neutron shielding characteristics of concretes containing different hematite proportions, Ann. Nucl. Energy 38 (2011) 2719-2723.

[48] A.M. El-Khayatt, I. Akkurt, Photon interaction, energy absorption and neutron removal cross section of concrete including marble, Ann. Nucl. Energy 60 (2013) 8-14.